

A “fast growth” method of computing free energy differences

D. A. Hendrix^a, C. Jarzynski^b

(a) *Physics Department, University of California, Berkeley, CA*

`dhendrix@socrates.berkeley.edu`

(b) *Theoretical Division, Los Alamos National Laboratory, Los Alamos, NM*

`chrisj@lanl.gov`

<http://qso.lanl.gov/~chrisj/>

Abstract

Let ΔF be the free energy difference between two equilibrium states of a system. An established method of numerically computing ΔF involves a single, long “switching simulation”, during which the system is driven reversibly from one state to the other (*slow growth*, or *adiabatic switching*). Here we study a method of obtaining the same result from numerous independent, *irreversible* simulations of much shorter duration (*fast growth*). We illustrate the fast growth method, computing the excess chemical potential of a Lennard-Jones fluid as a test case, and we examine the performance of fast growth as a practical computational tool.

LAUR-00-2050

INTRODUCTION

The development of numerical methods of computing the free energy difference $\Delta F = F^B - F^A$ between two equilibrium states of a system, A and B , is a field of active research^{1,2}, of significant practical importance in chemistry, physics, and biology. One widely applicable method – often called *slow growth* or *adiabatic switching* – utilizes a dynamical simulation during which the system evolves, maintained at a constant temperature, as an external parameter λ is slowly changed so as to drive the system from the initial to the final equilibrium state, $A \rightarrow B$. The evolution can occur as a sequence of discrete Monte Carlo steps, or as a time-continuous molecular dynamics trajectory. The slow growth method is often presented as a variant of *thermodynamic integration*³, with ΔF expressed as an integral over a continuous sequence of equilibrium states. However, slow growth can equally well be understood as the *in silico* exploitation of a basic result of statistical mechanics⁴:

$$\Delta F = W_\infty, \tag{1}$$

which states that the external work performed on a system during a reversible, isothermal process connecting two equilibrium states, is equal to the free energy difference between them. The slow growth method amounts to simulating such a “switching process” numerically, then equating the work performed with the desired free energy difference.

The subscript on W_∞ emphasizes that the process carrying the system from A to B is reversible, hence (in principle) of infinite duration. During such a process, the system evolves through a continuum of equilibrium states connecting A to B . In practice, exact reversibility is never achieved, and one uses a finite-time simulation to estimate the free energy difference:

$$\Delta F \approx W_\tau, \tag{2}$$

where W_τ denotes the work performed during a simulation of duration τ . The accuracy of a slow growth computation depends on how close one is to the reversible limit; for short switching times τ , the system can be driven far from equilibrium, resulting in a poor estimate of ΔF .

In recent years, the following *non-equilibrium work relation* has been derived^{5,6}, suggesting an alternative prescription for computing ΔF :

$$\exp(-\beta\Delta F) = \overline{\exp(-\beta W_\tau)}. \tag{3}$$

This result pertains to an *ensemble* of simulations of a switching process of *arbitrary* duration τ . The simulations are carried out independently, with initial conditions for the system sampled randomly from the canonical ensemble corresponding to the equilibrium state A . The work W_τ is computed for each simulation, and the overbar on the right denotes an average over the ensemble. The factor β is the inverse temperature of the initial equilibrium state, and also of the thermostat (see Section I below). Eq.3 can be rewritten as:

$$\Delta F = \lim_{N \rightarrow \infty} W_\tau^{x,N}, \tag{4}$$

where

$$W_\tau^{x,N} \equiv -\beta^{-1} \ln \left[\frac{1}{N} \sum_{n=1}^N \exp(-\beta W_{\tau,n}) \right]. \quad (5)$$

Here, $W_{\tau,n}$ is the work performed during the n 'th of N independent simulations. We will refer to $W_\tau^{x,N}$ as the *exponential average* of W_τ over the N simulations (in contrast with the ordinary average, which we will later introduce as $W_\tau^{a,N}$). We stress that the non-equilibrium work relation is valid for arbitrary τ . This is perhaps surprising: even for short switching times – for which the system is driven far from equilibrium, and the work performed during a typical simulation gives a sorry estimate of the free energy difference – we can still compute ΔF from the set of work values $\{W_{\tau,1}, W_{\tau,2}, \dots, W_{\tau,n}, \dots\}$ obtained from an ensemble of simulations.

Since $W_\tau^{x,N} \rightarrow \Delta F$ as $N \rightarrow \infty$ (with τ fixed), we are led to the following large- N approximation:

$$\Delta F \approx W_\tau^{x,N}. \quad (6)$$

Thus, after running many simulations of a given switching process, we can estimate ΔF as the exponential average of the values of work performed. We will refer to this proposed method of computing free energy differences as the *fast growth* method, to emphasize that it remains valid even for short switching times τ .

The aim of this paper is a study of the fast growth method. We have performed numerous switching simulations of the insertion of a single particle into a Lennard-Jones fluid, at various switching times τ . We will use the results of these simulations both to present an illustration of principle, and to examine the utility of fast growth as a practical computational method.

This paper is organized as follows. In Section I we briefly review the theoretical foundation of the fast growth method. In Section II we introduce our test case – the evaluation of the excess chemical potential of a Lennard-Jones fluid – and we present details of the computation. In Section III we use our numerical results to illustrate the validity of fast growth. In Section IV we use the same results to compare the slow and fast growth methods, given a fixed amount of computer time. Finally, in Section V we comment on the relationship between slow growth, fast growth, and a free energy formula based on the linear response approximation.

I. THEORETICAL BASIS OF FAST GROWTH

Here we introduce notation and briefly review the theoretical basis of the fast growth method. The emphasis will be on a presentation of the non-equilibrium work relation (Eq.3) oriented specifically toward the numerical problem of computing free energy differences. For a more physical presentation, see Ref.⁵.

Consider a system with a finite number of degrees of freedom, D . Let \mathbf{z} denote a point in the $2D$ -dimensional phase space of the system. Next, let λ denote an externally controlled parameter (for instance, an applied field), and let $H_\lambda(\mathbf{z})$ be the parameter-dependent Hamiltonian which gives the internal energy of the system, in terms of its microstate \mathbf{z} .

Now consider two equilibrium states of the system, A and B , defined at the same temperature, T , but corresponding to different values of the external parameter, λ^A and λ^B . The partition function associated with state A is given by the integral (assumed finite)

$$Z^A = \int d\mathbf{z} \exp[-\beta H^A(\mathbf{z})], \quad (7)$$

where $\beta = (k_B T)^{-1}$, and $H^A \equiv H_{\lambda^A}$; and similarly for state B . The free energy difference between the two states is then

$$\Delta F = F^B - F^A = -\beta^{-1} \ln \frac{Z^B}{Z^A}. \quad (8)$$

It is this quantity that we want to compute.

Next, suppose we choose a *thermostating scheme*, a numerical prescription for generating evolution under which our system samples the canonical ensemble associated with any equilibrium state (λ, T) . Intuitively, we can view the thermostating scheme as a way of “mocking up” the evolution of a system in contact with a heat reservoir. This evolution might take the form of a continuous-time trajectory, or a discrete sequence of Monte Carlo steps. Examples of such schemes include the Metropolis Monte Carlo algorithm⁷, Langevin dynamics, the Andersen thermostat⁸, and the Nosé-Hoover thermostat^{9,10}. Note that the thermostating scheme is itself parametrized by (λ, T) (e.g. the Metropolis acceptance probability takes the form $e^{-\beta H_\lambda}$), and might be explicitly *stochastic*, relying on the generation of random numbers to produce the evolution.

Imagine that we now run a simulation, first sampling the initial microstate of our system from the canonical ensemble corresponding to state A , then letting the system evolve in time under the thermostating scheme, as the value of λ is externally changed – or “switched” – from λ^A to λ^B , and the temperature of the thermostat is held fixed at T . For continuous-time evolution, let τ denote the duration of the simulation; let $\lambda(t)$ specify the (externally imposed) parametric time-dependence, from $\lambda(0) = \lambda^A$ to $\lambda(\tau) = \lambda^B$; and consider the integral

$$W_\tau = \int_0^\tau dt \dot{\lambda}(t) \frac{\partial H_\lambda}{\partial \lambda}(\mathbf{z}(t)), \quad (9)$$

where $\dot{\lambda} = d\lambda/dt$, and $\mathbf{z}(t)$ represents the evolution of the system. Alternatively, if the evolution is implemented with an explicitly discrete algorithm (e.g. Metropolis Monte Carlo), then the corresponding quantity is

$$W_\tau = \sum_{t=0}^{\tau-1} [H_{\lambda_{t+1}}(\mathbf{z}_t) - H_{\lambda_t}(\mathbf{z}_t)], \quad (10)$$

where \mathbf{z}_t is the microstate of the system and λ_t the value of the parameter, after t steps; and τ is the total number of steps in the simulation. In what follows, we will use the notation of continuous-time evolution, but the statements apply to explicitly discrete evolution as well.

The quantity W_τ can be interpreted as the external *work* performed on the system over the course of the simulation.^{5,4,11–14} We will use this interpretation, though we warn the reader that Eq.9 (or Eq.10) is by no means an accepted, textbook definition of work, and

the interpretation of W_τ as work may be subject to dispute. The results presented, however, do not depend on the validity of this interpretation.

The trajectory $\mathbf{z}(t)$ which emerges from our simulation (and which in turn determines the value of W_τ) depends on a string of random numbers: those involved in sampling the initial conditions, as well as those, if any, needed to generate the evolution itself. By repeating the simulation with different sets of random numbers, we obtain different *realizations* of the process we are simulating. We view these as representing independent samples from an infinite ensemble of all possible realizations.¹⁵ Eq.3 then states that the average value of $e^{-\beta W_\tau}$ over the ensemble of possible realizations is equal to $e^{-\beta \Delta F}$, with ΔF as given by Eq.8. In other words, $e^{-\beta W_\tau}$ is an *unbiased estimator* of $e^{-\beta \Delta F}$. By collecting sufficiently many samples from the ensemble of realizations (i.e. by repeatedly running simulations) we can in principle compute the average of $e^{-\beta W_\tau}$ to the desired degree of accuracy. This is the essence of the fast growth method.

For a variety of thermostating schemes, Eq.3 has been established as an exact result, valid for any finite switching time τ . Precise conditions under which this result is rigorously true are presented in Refs.^{6,13}. In particular, all four thermostating schemes mentioned earlier – Metropolis, Langevin, Andersen, Nosé-Hoover – satisfy these conditions.

Note that we do not automatically gain something for nothing with the fast growth method: while it allows us to compute ΔF without the bother of running a very long simulation, the price paid is that many short simulations might be needed.

Finally, we mention that, in the limit $\tau \rightarrow 0$, Eq.3 reduces to the well-known *free energy perturbation* identity¹⁶:

$$\exp(-\beta \Delta F) = \langle \exp(-\beta \Delta H) \rangle_A, \quad (11)$$

where $\Delta H \equiv H^B - H^A$ is the difference between the two Hamiltonians, evaluated at a given microstate; and $\langle \cdots \rangle_A$ denotes an average over microstates sampled from the canonical ensemble A .

II. TEST CASE: EXCESS CHEMICAL POTENTIAL OF A LENNARD-JONES FLUID

To illustrate the fast growth method, we chose to compute the excess chemical potential of a three-dimensional Lennard-Jones fluid. This is equal to the free energy change associated with “turning on” the interactions between a single particle and the remainder of the fluid, at constant volume and temperature¹. This process can be viewed as the transfer of one particle from an ideal gas to the Lennard-Jones fluid; the *excess* chemical potential is defined as the chemical potential of the fluid relative to that of the ideal gas. Following the notation of Mon and Griffiths¹⁷, let U_M denote the potential energy of M identical, classical particles interacting pairwise:

$$U_M(\mathbf{r}_1, \cdots, \mathbf{r}_M) = \sum_{i < j} \Phi(|\mathbf{r}_j - \mathbf{r}_i|), \quad (12)$$

where Φ is the interaction potential. Now imagine a system of $M + 1$ particles, and consider two Hamiltonians:

$$H^A(\mathbf{z}) = \sum_{i=1}^{M+1} \frac{p_i^2}{2m} + U_M(\mathbf{r}_1, \dots, \mathbf{r}_M) \quad (13)$$

$$H^B(\mathbf{z}) = \sum_{i=1}^{M+1} \frac{p_i^2}{2m} + U_{M+1}(\mathbf{r}_1, \dots, \mathbf{r}_{M+1}). \quad (14)$$

In both cases \mathbf{z} is the $6(M+1)$ -dimensional vector specifying the positions and momenta of all the particles. H^A describes M interacting particles, plus a “tagged” particle moving freely; H^B describes $M+1$ interacting particles. We take the positions \mathbf{r}_i to be confined within a cube of volume $V = L^3$ with periodic boundary conditions. Note that the difference

$$\Delta H \equiv H^B - H^A = \sum_{i=1}^M \Phi(|\mathbf{r}_{M+1} - \mathbf{r}_i|) \equiv \Psi(\mathbf{r}_1, \dots, \mathbf{r}_{M+1}) \quad (15)$$

is just the interaction energy between the tagged particle and the others.

At a given temperature T , Eqs.7 and 8 define partitions functions Z^A and Z^B , and the free energy difference ΔF , for the Hamiltonians H^A and H^B . This free energy difference, i.e. the work associated with reversibly turning on the interaction Ψ at constant V and T , is the excess chemical potential:

$$\mu_{ex} = \Delta F \quad (16)$$

Let us now parametrize a *family* of Hamiltonians, $H_\lambda(\mathbf{z})$, interpolating linearly from H^A to H^B :

$$H_\lambda = H^A + \lambda\Psi, \quad (17)$$

so that $H^A = H_0$ and $H^B = H_1$. The intermediate Hamiltonians ($0 < \lambda < 1$) represent a partially interacting tagged particle.

A switching simulation then proceeds as follows. We start by sampling initial conditions from the canonical ensemble corresponding to H^A . We then allow the $(M+1)$ -particle system to evolve in time under a chosen thermostating scheme, as λ is switched from 0 to 1 over a time τ , i.e. from a non-interacting to a fully interacting tagged particle. By running either a single simulation with τ very large (slow growth), or many simulations with smaller τ (fast growth), we can construct an estimate of μ_{ex} from the value(s) of external work, W_τ , performed during the simulation(s), using Eq.2 or 6.

At the end of Section I, we alluded to the fact that, in the limit $\tau \rightarrow 0$, fast growth reduces to the free energy perturbation method of computing ΔF . For the particular case considered here, this is equivalent to Widom’s *particle insertion method*^{1,18}, which gives μ_{ex} in terms of sampled values of the energy cost (ΔH) of suddenly materializing an additional particle at a randomly chosen location within the fluid.

We performed switching simulations at various switching times τ . The results of these will be presented in the following section. Here we describe the details and parameters of the simulations themselves.

The usual Lennard-Jones interaction potential, for a pair of particles separated by a distance r , is given by

$$\Phi_{LJ}(r) = 4\epsilon \left[\left(\frac{\sigma}{r} \right)^{12} - \left(\frac{\sigma}{r} \right)^6 \right], \quad (18)$$

where ϵ is the depth of the potential at its minimum, and σ is the van der Waals diameter of the particle. We instead used a modified potential:

$$\Phi(r) = \begin{cases} a - br^2 & 0 \leq r \leq 0.8\sigma \\ \Phi_{LJ}(r) + c(r - r_c) - d & 0.8\sigma \leq r \leq r_c \\ 0 & r_c \leq r. \end{cases} \quad (19)$$

Here r_c is a cutoff distance, which we took to be half the length of a side of the box:

$$r_c = L/2. \quad (20)$$

and the constants a , b , c , and d were chosen to preserve the continuity of Φ and its derivative. We used $\Phi(r)$ rather than $\Phi_{LJ}(r)$ both to avoid the singularity at $r = 0$, and to impose a strict radius of interaction equal to $L/2$. The need for the latter condition arose from our use of periodic boundary conditions, which is equivalent to an infinite lattice of identical cells: the requirement that Φ vanish for $r > L/2$ guarantees that, given a pair of particles, each interacts only with a single image of the other.

For the parameter values we have chosen, the difference between $\Phi(r)$ and $\Phi_{LJ}(r)$ is very small for $r > 0.8\sigma$. Furthermore, we have found the core repulsion between particles to be sufficiently strong that two fully interacting particles will essentially never come closer than a distance 0.8σ of one another. These considerations suggest that the excess chemical potential μ_{ex} which we plan to compute will differ little from that defined for the usual Lennard-Jones fluid. However, this issue is not particularly relevant for the central aim of this paper.

Since the Lennard-Jones potential works especially well with inert gases, we modeled an argon fluid. The parameters associated with argon are¹⁹

$$\sigma = 3.542 \times 10^{-10} \text{m} = 3.542 \text{ \AA} \quad (21)$$

$$\epsilon = 1.288 \times 10^{-21} \text{J} = 0.1854 \text{ kcal/mol} \quad (22)$$

$$m = 6.634 \times 10^{-26} \text{kg} = 39.94 \text{ amu.} \quad (23)$$

We took these values to define the units of length, energy, and mass in our simulation. The units for time and temperature are then: $\sigma\sqrt{m/\epsilon} = 2.542 \text{ps}$ and $\epsilon/k_B = 93.3 \text{K}$, respectively. Henceforth, all values will be quoted in these units.

We chose the *Andersen thermostat*⁸ to simulate the effects of an external heat reservoir. In this scheme, the evolution of the fluid is governed by Newton's equations, supplemented by the forced thermalization of the momenta of randomly chosen particles, at regular intervals. Specifically, at fixed time intervals δt_{And} , a particle is chosen at random, and all three components of its momentum vector are replaced by *thermal* values, sampled randomly from the Maxwell-Boltzmann momentum distribution at the thermostat temperature T . To carry out the integration of Newton's equations, we used the velocity-Verlet algorithm¹.

All of our simulations were run using $M = 125$ untagged particles, plus one tagged particle, inside a box of sides $L = 5.3$, with the thermostat set at $T = 1$.

During each switching simulation (following a relaxation interval at $\lambda = 0$, to generate an initial equilibrium microstate; see Section IV), the interaction strength of the untagged particle was turned on according to the schedule:

$$\lambda(t) = (t/\tau)^2, \quad (24)$$

from $t = 0$ to $t = \tau$. The time step for the velocity-Verlet integration was taken to be $\delta t_{\text{Ver}} = .01$, and the Andersen momentum thermalization was implemented at every time step: $\delta t_{\text{And}} = .01$.

III. RESULTS: ILLUSTRATION OF PRINCIPLE

We ran a varying number of simulations of the switching process, at seven different values of the switching time, from $N = 3334$ simulations at $\tau = 3.0$, to $N = 10$ simulations at $\tau = 1000.0$, keeping the total switching time devoted to each set of simulations, $N\tau$, fixed at (approximately) 10^4 . For every simulation, we computed the work performed as a result of turning on the interactions between the tagged particle and the rest. We then calculated both the ordinary and exponential average of these values of work, over the simulations corresponding to each value of τ :

$$W_\tau^{a,N} = \frac{1}{N} \sum_{n=1}^N W_{\tau,n} \quad (25)$$

$$W_\tau^{x,N} = -\beta^{-1} \ln \left[\frac{1}{N} \sum_{n=1}^N \exp(-\beta W_{\tau,n}) \right], \quad (26)$$

where $W_{\tau,n}$ denotes the work performed during the n 'th simulation of duration τ .

The results are summarized in Fig.1. The error bars on the exponential averages (circles) were computed with the bootstrap method²⁰. Error bars on the ordinary averages (squares) are not shown, but were typically the size of the squares themselves.

Additionally, we performed two very long simulations at $\tau = 25000.0$, and used the average of these as our best estimate of the true value of ΔF (defined by Eq.8). This is shown as the horizontal line at $W = 1.174$ in Fig.1, and – judging from the difference between these two (nearly quasi-static) simulations – this value should be understood to have an uncertainty of ~ 0.1 .

Let us now consider the salient features of Fig.1, beginning with the values of $W_\tau^{a,N}$. If we view the work performed during a single simulation, W_τ , to be an estimate of the free energy difference ΔF , then this estimate is subject to both statistical and systematic errors^{21–23}. The former reflect the *spread* in the distribution of W_τ values (for a given τ), the latter a *bias*: W_τ tends to over-estimate ΔF . This bias follows rigorously from the non-equilibrium work relation⁵, but can also be understood in terms of thermodynamic considerations^{4,24} (e.g. the Second Law), if one accepts the interpretation of W_τ as work. By averaging W_τ over infinitely many realizations, the statistical error is removed, but the systematic error remains:

$$\lim_{N \rightarrow \infty} W_\tau^{a,N} = \overline{W_\tau} > \Delta F \quad (\text{finite } \tau). \quad (27)$$

Thus, for any value of τ , the quantity $\overline{W_\tau} - \Delta F$ represents the *systematic error* associated with using simulations of duration τ to estimate ΔF . As expected, this error (approximated by $W_\tau^{a,N} - \Delta F$ in Fig.1) is positive, but decreases as we approach the reversible limit, $\tau \rightarrow \infty$.

The *exponential average* of W_τ over N simulations of duration τ , viewed as an estimate of ΔF , also contains errors when N is finite⁶, but these are removed in the limit of infinitely many simulations:

$$\lim_{N \rightarrow \infty} W_\tau^{x,N} = \Delta F \quad (\text{arbitrary } \tau). \quad (28)$$

The values of $W_\tau^{x,N}$ shown in Fig.1 are consistent with this statement. All of the exponential averages closely approximate (our best estimate of) the free energy difference, $\Delta F = 1.174$, illustrating the validity of the fast growth method.

The histogram in Fig.2 displays the distribution of work values for the set of simulations performed at $\tau = 3.0$. The three vertical lines show the locations of the ordinary average of the work values, $W^a = 8.413$, the exponential average, $W^x = 1.478$, and the free energy difference, $\Delta F = 1.174$, shown in Fig.1. (Throughout the paper, we frequently suppress the subscript τ and/or the superscript N .) Note that W^x and ΔF are quite close: despite values of W ranging from -4.3 to $+34.1$, the exponential average W^x differs from ΔF by only ~ 0.3 , which is not much larger than our uncertainty in the value of ΔF itself!

Figs.1 and 2 are intended as an “illustration of principle” of the fast growth method, demonstrating that the value of ΔF can be extracted from an ensemble of finite-time switching simulations, during which the system is explicitly driven away from equilibrium.

IV. COMPARISON OF METHODS

Both slow and fast growth converge to the correct value of ΔF in the limit of infinite computational resource: $\tau \rightarrow \infty$ for slow growth, $N \rightarrow \infty$ for fast growth. In practice, of course, we can perform neither a single infinitely long simulation, nor infinitely many finite-time simulations, so it becomes interesting to pose the following question: Given a *finite* amount of computer time, which method is preferable? We now consider this question empirically, in a manner relevant to the practical computation of free energy differences. Specifically, we study how the accuracy of the predicted free energy difference depends on the choice of the switching time, τ , given a fixed amount of total computational time.

Imagine that we have been allotted τ_{TOT} units of simulation time. In this total we must include not only the time devoted to repetitions of the switching process itself, but also the time used to generate a microstate sampled from equilibrium, before the start of each process. If each switching realization is preceded by a relaxation interval of duration τ_{REL} (to generate the initial microstate), then the number of switching realizations possible is given by the largest integer N satisfying the inequality:

$$N \leq \frac{\tau_{\text{TOT}}}{\tau_{\text{REL}} + \tau}. \quad (29)$$

In the simulations described in Section III, for each value of τ the results were obtained from a single, long run, in which realizations of the switching process itself alternated with relaxation intervals of duration $\tau_{\text{REL}} = 1.0$, during which the system evolved at fixed $\lambda = 0$. (The final microstate at the end of a given switching simulation was taken as the seed for the following relaxation interval.²⁵ The value of τ_{REL} was chosen on the basis of simulations showing that correlations in our system decay to zero over ~ 0.6 time units.) We used these

results to investigate predictions of ΔF for various switching times τ , given a total resource of $\tau_{\text{TOT}} = 1050.0$ time units of simulation. For each of the seven switching times considered, we generated ten predictions of ΔF using the data from the simulations. For instance, at $\tau = 5.0$, Eq.29 gives $N = 175$; therefore, of the 2000 switching realizations performed at $\tau = 5.0$, we used the first 1750 to generate ten independent estimates of ΔF . The remaining 250 realizations were not used here.

Fig.3 displays the results, for the various switching times. Each circle represents an estimate of ΔF obtained from a total of (no more than) 1050.0 units of simulation time. The data at $\tau = 1000.0$ are slow growth estimates ($N = 1$), whereas the remaining points make explicit use of the fast growth formula (Eq.5). A striking feature of these results is that the accuracy of the predictions does not seem to depend drastically on τ . In other words, for the example considered in this paper, *fast growth and slow growth yield comparably good estimates of ΔF for a fixed computational resource, over a wide range of switching times.*

Additionally, we generated ten estimates of ΔF using the Widom method – shown as crosses at $\tau = 0.0$ – again with a total of 1050.0 time units devoted to each estimate. Here, however, we effectively took $\tau_{\text{REL}} = 0.1$: after every time interval $\Delta t = 0.1$, we generated a random location for the $(M + 1)$ 'th particle, determined ΔH , and then continued with the simulation of $M = 125$ mutually interacting particles. Thus, 10500 samples of ΔH contributed to each of the ten Widom estimates. As we made no attempt to optimize Δt , these results do not really represent a direct and fair comparison between fast growth and the Widom method, and rather serve as an illustration of the latter.

In the asymptotic limit of large N and large τ , Crooks²⁶ has shown that the size of errors in the estimate of ΔF depends only on $N\tau$. On the other hand, for fast switching, the distribution of work values can become quite wide, resulting in slow convergence of $W_\tau^{x,N}$ with N . This is a well-known problem associated with computing exponential averages (as with the free energy perturbation method²²), which manifests itself both in large statistical errors, and – if the distribution is wide enough – as a significant bias toward over-estimation of ΔF . The Widom data ($\tau = 0.0$) certainly shows these symptoms; the somewhat wide scatter of predictions at $\tau = 3.0$ is likely also evidence of this problem.

We suspect that, generically, the expected error associated with fast growth decreases with increasing τ (for fixed τ_{TOT}). If this is indeed the case, then Fig.3 suggests that for $\tau \geq 5.0$ this trend is lost in the noise; any gain in accuracy obtained by using one switching realization of duration 1000.0 rather than 175 realizations of duration 5.0, is likely to be smaller than the unavoidable statistical error associated with trying to compute ΔF with a finite resource of 1050.0 units of simulation time.

The above, tentative conclusion – that for a given τ_{TOT} the accuracy does not depend strongly on τ , over a wide range of switching times – suggests a certain advantage of fast growth over slow growth as a practical computational tool. Namely, fast growth allows for the immediate estimation of errors²⁶, both statistical and systematic. Using the N values of work obtained from different switching realizations, the statistical uncertainty in the average of $e^{-\beta W_\tau}$ – the unbiased estimate of $e^{-\beta \Delta F}$ – can be ascertained in the usual way, in terms of the variance; the resulting upper and lower bounds defining the error bar then translate immediately into lower and upper bounds on the estimate of ΔF itself. Alternatively, one can use the bootstrap method²⁰, which is sensitive to the possibility that the exponential average might be dominated by one or a few particularly small values of work, out of the N

values obtained from the switching realizations. Slow growth, by contrast, produces only a single value of work, which by itself provides no estimate of its own error!

In addition to statistical errors, the fast growth estimate contains a systematic bias: for finite N , $W_\tau^{x,N}$ tends to over-estimate ΔF , though to a lesser degree than $W_\tau^{a,N}$ ⁶. This bias has the same origin as the “sample-size hysteresis” studied in the context of the free energy perturbation method, and Eq.10 of Ref.²² gives us a leading-order estimate of its size:

$$\overline{W_\tau^{x,N}} - \Delta F \approx \beta \sigma_W^2 / 2N. \quad (30)$$

Here the overbar denotes an expectation value (i.e. the average over infinitely many attempts to estimate ΔF with N values of W , using fast growth), and σ_W^2 is the variance in the work values. Note that this bias vanishes as $N \rightarrow \infty$, as demanded by consistency with Eq.4.

For each of the fast growth estimates shown in Fig.3, we have estimated both the statistical uncertainty (using the bootstrap method) and the systematic bias (using Eq.30). We found that the latter never exceeded 0.07, and that the estimated statistical uncertainty was typically about an order of magnitude greater than the estimated bias. These conclusions are in agreement with Fig.3, which visually suggests that statistical rather than systematic errors dominate our fast growth predictions.

With fast growth, the easy estimation of error bars can furthermore be harnessed to determine, “on the fly”, the optimal amount of computer time to devote to the estimation of ΔF : the user simply performs one simulation after another, updating both $W_\tau^{x,N}$ and its error bar after each simulation, and stops when the size of the error becomes satisfactorily small. With slow growth, one must estimate ahead of time how long the simulation needs to be, given the desired accuracy.

Our discussion so far has been implicitly oriented toward the computation of free energy differences on *single-processor* computers, where easy estimation of statistical errors seems to be the main advantage of fast growth over slow growth. However, on parallel machines another considerable advantage emerges: fast growth is *embarrassingly parallelizable*. Given P processors and a finite amount of dedicated run time, the user simply lets each processor perform one or more switching simulations, and at the end all the values of work are gathered and the exponential average is computed. This provides the maximal efficiency of parallelization, $\sim 100\%$, as there is essentially no “cross-talk” between processors. Furthermore, the additional programming effort is minimal: once a code has been written to perform switching simulations on a single processor, little more needs to be done to let P copies of the code run independently on P processors. By contrast, to efficiently distribute a single simulation over P processors requires considerable programming skills and time, and the optimal parallelization scheme may well depend on details of the hardware – e.g. are the processors divided into shared-memory clusters?, how fast is the communication between different processors?, etc. – making it less portable.

The fast growth method is particularly well-suited for Beowulf-type clusters, built at relatively low cost with off-the-shelf hardware components. In such clusters, the processors typically do not share memory, and communication between them is often relatively slow. Both drawbacks are avoided by any embarrassingly parallelizable method such as fast growth.

V. FAST GROWTH, SLOW GROWTH, AND LINEAR RESPONSE

The idea of computing ΔF from numerous values of W_τ is not new. Indeed, it has been recognized for some time that, in the interest of having an estimate of statistical errors, several or more independent switching simulations should be carried out²¹.

Given a number of independent values of W_τ , the simplest imaginable approximation of ΔF – though clearly not the best (Fig.1) – is just the ordinary average of these values:

$$\Delta F \approx W_\tau^a \quad (31)$$

This amounts to slow growth, with statistical errors reduced by averaging over samples. In 1991, Hermans²³ suggested instead the following formula:

$$\Delta F \approx W_\tau^a - \beta\sigma_W^2/2, \quad (32)$$

where σ_W^2 is the variance of the set of work values (closely related results are found in Wood *et al*²², and – for isolated systems – in Tsao *et al*²⁴). This result can be viewed as a fluctuation-dissipation relation, and therefore ought to be valid in the *linear response* regime, i.e. when λ is switched slowly enough that the system remains near equilibrium for the duration of the process.

Eq.32 represents a correction to Eq.31, aiming to compensate for the systematic error (see Section III) inherent in using W_τ as an estimate of ΔF . Thus we can expect $W_\tau^a - \beta\sigma_W^2/2$ to give a better estimate of ΔF than W_τ^a , *in the regime of validity of linear response*. Using the work values obtained from the simulations described in Section III, we have compared – for various switching times – three estimates of ΔF : W_τ^a (corresponding to slow growth, with the statistical error reduced by averaging), $W_\tau^a - \beta\sigma_W^2/2$ (linear response), and W_τ^x (fast growth). Fig.4 displays the results. As expected, there exists a near-equilibrium regime (roughly, $\tau \geq 20.0$) in which linear response does a good job of removing the systematic error inherent in using W_τ as an estimate of ΔF . For shorter times, however, linear response breaks down, as the system is driven significantly away from equilibrium. Fig.4 furthermore illustrates that the non-equilibrium work relation is truly a *far-from-equilibrium* result, remaining valid even outside the regime of validity of the near-equilibrium prediction (Eq.32).

The relationship between the three estimates considered in Fig.4 can be understood by rewriting Eq.3 as follows⁵:

$$\Delta F = \sum_{n=1}^{\infty} (-\beta)^{n-1} \frac{\omega_n}{n!}, \quad (33)$$

where ω_n is the n 'th cumulant of the distribution of values of W . Keeping only the first term on the right side gives us $\Delta F \approx W_\tau^a$, whereas keeping two terms yields the linear response approximation, $\Delta F \approx W_\tau^a - \beta\sigma_W^2/2$. Therefore these approximations can be viewed as the first two in an expansion derived from the non-equilibrium work relation, Eq.3.

Note that one can justify keeping only the first two terms in the cumulant expansion, by assuming a Gaussian distribution of work values: since all higher ($n > 2$) cumulants vanish for a Gaussian, Eq.33 reduces to Eq.32 in that case. More directly (i.e. without resorting to a cumulant expansion), it is easily verified that for an assumed Gaussian distribution of work

values, Eq.3 implies a relationship between the mean and the variance of the distribution, namely $\Delta F = \overline{W} - \beta\sigma_W^2/2$.

It is easy to argue heuristically that a Gaussian distribution of work values emerges in the linear response regime, i.e. when the switching is slow enough (τ large enough) to keep the system near equilibrium. Namely, we can imagine that the work W , for one simulation, becomes a sum of many independent contributions: if we break the long time interval $0 < t < \tau$ into many shorter segments – each, however, longer than the correlation time associated with the dynamics of the system – then the contributions to W_τ from the various segments will be (roughly) independent. The central limit theorem (CLT) then leads us to expect that, given many realizations of this process, the distribution of work values, $\rho(W)$, will be approximately Gaussian. However, this argument requires some care: if the spread in the values of W is large ($\sigma_W \gg k_B T$), then the dominant contribution to $\int \rho e^{-\beta W}$ comes from values in the (lower) *tail* of $\rho(W)$, precisely where the CLT “breaks down”²⁷. So a more careful justification invoking the CLT (to derive Eq.32 from Eq.3) requires also that σ_W be not much larger than $k_B T$. This will be satisfied for sufficiently slow switching, since $\rho \rightarrow \delta(W - \Delta F)$ as $\tau \rightarrow \infty$ (Eq.1). Hence, the argument is ultimately justified.

CONCLUSIONS

In this paper, we have studied the fast growth method, applying it to compute the excess chemical potential of a (modified) Lennard-Jones fluid. Figs.1 and 2 illustrate the validity of the method, showing that it accurately estimates ΔF over a wide range of switching times, including short times for which the system is driven far from equilibrium. Moreover, Fig.3 suggests that the accuracy of the prediction does not depend strongly on the choice of τ (for a fixed total computational resource), again over a wide range of values. However, when τ is too short, then fast growth becomes susceptible to the problem of poor convergence of exponential averages, familiar to any practitioner of the free energy perturbation method (which in the present context is the Widom particle insertion method). Finally, we have considered the relationship between fast growth and the linear response approximation.

The natural question left open by our study is: How generally valid are the results which we have found empirically? In particular, how robust is the conclusion about relative performance of slow and fast growth, i.e. “comparable accuracy for equal computational resource”? If this conclusion is indeed generally true, then it suggests certain advantages for fast growth (easy estimation of errors, parallelizability).

Finally, it is likely that fast growth can be improved by combining it with strategies which have been studied in the context of the free energy perturbation (Eq.11). Suggestions to this end have included the overlapping distributions method²⁸, higher-order cumulant expansions²⁹, and averaging of forward and reverse processes³⁰.

ACKNOWLEDGMENTS

The authors are grateful for stimulating discussions with Tanmoy Bhattacharya, Daan Frenkel, Angel Garcia, Jan Hermans, Gerhard Hummer, Lawrence Pratt, Mike Warren, and Robert Wood, as well as scrupulous and useful commentary by an anonymous referee. This

research is supported by the Department of Energy, under contract W-7405-ENG-36. D.A.H. furthermore acknowledges the support of the 1999 Los Alamos Summer School program.

REFERENCES

- ¹ D.Frenkel, B.Smit, *Understanding Molecular Simulation: From Algorithms to Applications*, Academic Press, San Diego (1996). Chapter 7 is devoted to free energy computation methods.
- ² For a sampling of free energy methods developed during the 1990's, see M.Watanabe and W.P.Reinhardt, *Phys.Rev.Lett.***65**, 3301 (1990); B.A.Berg and T.Neuhaus, *Phys.Lett.B* **267**, 249 (1991); B.L.Holian, H.A.Posch, and W.G.Hoover, *Phys.Rev.E* **47**, 3852 (1993); T.C.Beutler and W.F.van Gunsteren, *J.Chem.Phys.***101**, 1417 (1994); X.Kong and C.L.Brooks III, *J.Chem.Phys.***105**, 2414 (1996); A.D.Bruce, N.B.Wilding, and G.J.Ackland, *Phys.Rev.Lett.***79**, 302 (1997); R.J.Radmer, P.A.Kollman, *J.Comp.Chem.***18**, 902 (1997); M.deRoning, A.Antonelli, S.Yip, *Phys.Rev.Lett.***83**, 3973 (1999); J.R.Gullingsrud, R.Braun, K.Schulten, *J.Comp.Phys.***151**, 190 (1999); R.H.Wood *et al*, *J.Chem.Phys.***110**, 1329 (1999); as well as references listed below.
- ³ J.G.Kirkwood, *J.Chem.Phys.***3**, 300 (1935).
- ⁴ W.P.Reinhardt and J.E.Hunter III, *J.Chem.Phys.***97**, 1599 (1992); J.E.Hunter III, W.P.Reinhardt, T.F.Davis, *J.Chem.Phys.* **99**, 6856 (1993).
- ⁵ C.Jarzynski, *Phys.Rev.Lett.***78**, 2690 (1997).
- ⁶ C.Jarzynski, *Phys.Rev.E* **56**, 5018 (1997).
- ⁷ N.Metropolis *et al.*, *J.Chem.Phys.* **21**, 1087 (1953).
- ⁸ H.C.Andersen, *J.Chem.Phys.* **72**, 2384 (1980).
- ⁹ S.Nosè, *J.Chem.Phys.* **81**, 511 (1984).
- ¹⁰ W.G.Hoover, *Phys.Rev. A* **31**, 1695 (1985).
- ¹¹ K.Sekimoto, *Prog.Theor.Phys.Suppl.* **130**, 17 (1998).
- ¹² C.Jarzynski, *Acta Phys.Polonica B* **29**, 1609 (1998).
- ¹³ G.E.Crooks, *J.Stat.Phys.* **90**, 1481 (1998).
- ¹⁴ The essence of this interpretation seems to date back to Erwin Schrödinger's lectures: *Statistical Thermodynamics* (Cambridge, 1962). See the paragraphs found between Eqs.2.13 and 2.14.
- ¹⁵ In a laboratory experiment (as opposed to a computer simulation) differences between one realization of the switching process and the next arise from differences in microscopic initial conditions sampled for both the system and the heat reservoir⁵.
- ¹⁶ R.Zwanzig, *J.Chem.Phys.***22**, 1420 (1954).
- ¹⁷ K.K. Mon, R.B. Griffiths, *Phys.Rev.A* **31**, 956 (1985)
- ¹⁸ B.Widom, *J.Chem.Phys.* **39**, 2802 (1963).
- ¹⁹ R.Reid, J.Prausnitz, T.Sherwood, *The Properties of Gases and Liquids*, 3rd ed., App. A and C. McGraw-Hill, New York (1977).
- ²⁰ B.Efron, *The Jackknife, the Bootstrap and Other Resampling Plans*, Society for Applied Mathematics, Philadelphia (1982).
- ²¹ M.J.Mitchell and J.A.McCammon, *J.Comp.Chem.***12**, 271 (1991).
- ²² R.H.Wood, W.C.F.Mühlbauer, P.T.Thompson, *J.Phys.Chem.***95**, 6670 (1991).
- ²³ J.Hermans, *J.Phys.Chem.***95**, 9029(1991)
- ²⁴ L.-W.Tsao, S.-Y.Sheu, and C.-Y.Mou, *J.Chem.Phys.***101**, 2302 (1994).
- ²⁵ Alternatively, the initial microstate could have been used.
- ²⁶ G.E.Crooks, *Excursions in Statistical Dynamics*, Ph.D. Thesis, U.C. Berkeley, Dept. of Chemistry, 1999; Section 4.3.

²⁷ D.J.Searles and D.J.Evans, *J.Chem.Phys.***112**, 9727 (2000).

²⁸ D.Frenkel, private communication.

²⁹ G.Hummer, private communication.

³⁰ J.Hermans, private communication.

FIGURES

FIG. 1. For each of the seven sets of simulations, corresponding to switching times from $\tau = 3.0$ to 1000.0, we computed both the ordinary average (W^a) and the exponential average (W^x) of the work values. These are shown in the figure, along with our estimate for the true value of ΔF , the solid line at $W = 1.174$. The ordinary averages, W^a , displayed as squares, over-estimate ΔF , although the difference decreases as one approaches the reversible limit. By contrast, the exponential averages W^x (circles) provide significantly better estimates of ΔF . The number of simulations, N , performed for each value of the switching time, τ , was chosen so that $N\tau = 10000.0$ in each case (except $N\tau = 10002.0$ for $\tau = 3.0$).

FIG. 2. A histogram, showing the distribution of values of W , in bins of unit energy width, for the 3334 simulations performed at the shortest switching time, $\tau = 3.0$. The three vertical lines show the ordinary average of these work values, W^a , the exponential average, W^x , and (our best estimate of) the free energy difference, ΔF .

FIG. 3. Each circle or cross represents an estimate of ΔF , using no more than 1050.0 units of simulation time. The ten circles at $\tau = 1000.0$ are thus slow growth estimates; all other circles are fast growth estimates; and the crosses at $\tau = 0.0$ were obtained with the Widom method.

FIG. 4. The squares, circles, and diamonds show three sets of estimates of ΔF : W^a , W^x , and $W^a - \beta\sigma_W^2/2$, respectively. These estimates were obtained from the same data used in the previous figures, i.e. the squares and circles are the those shown in Fig.1.

Figure 1

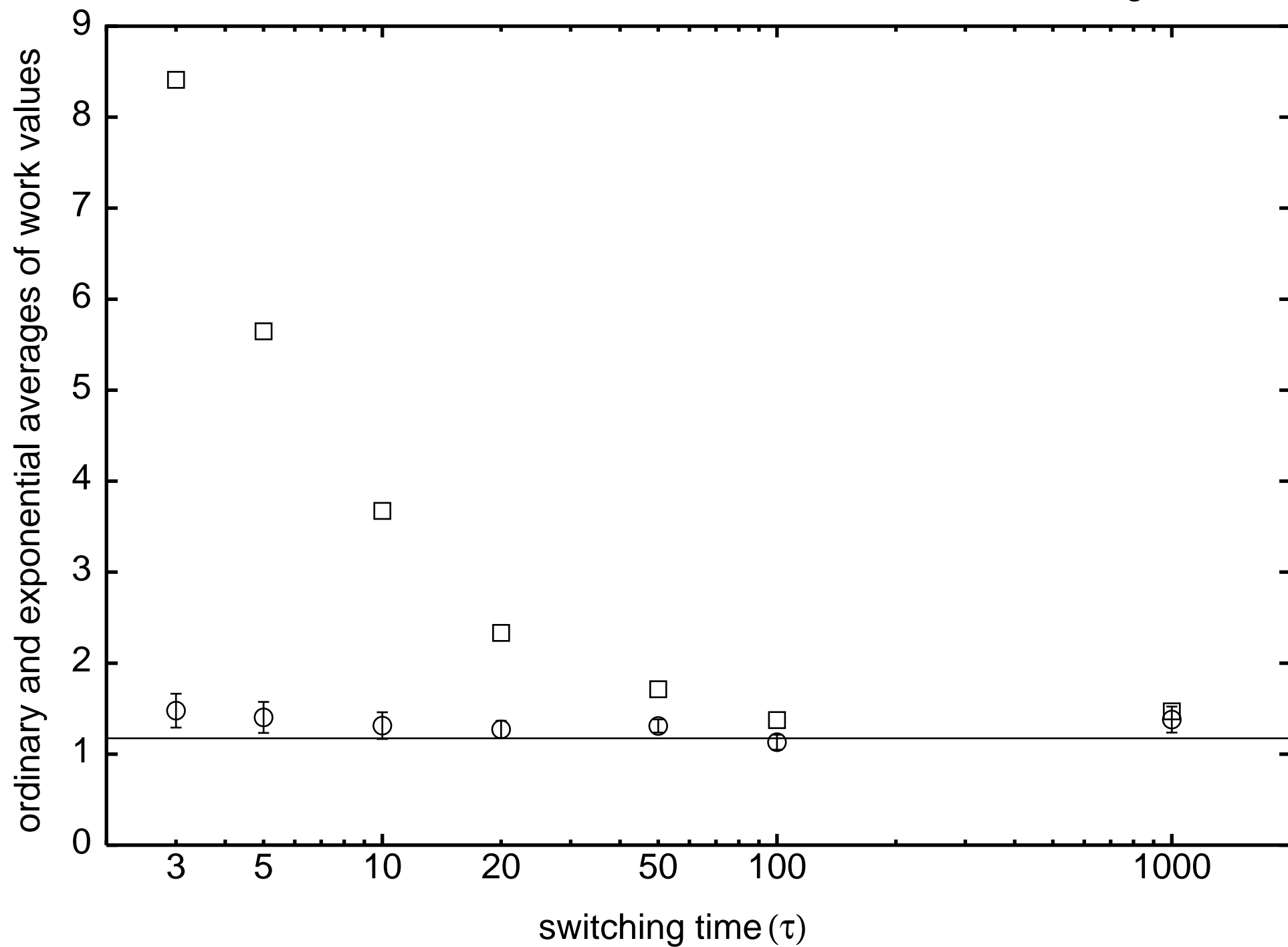


Figure 2

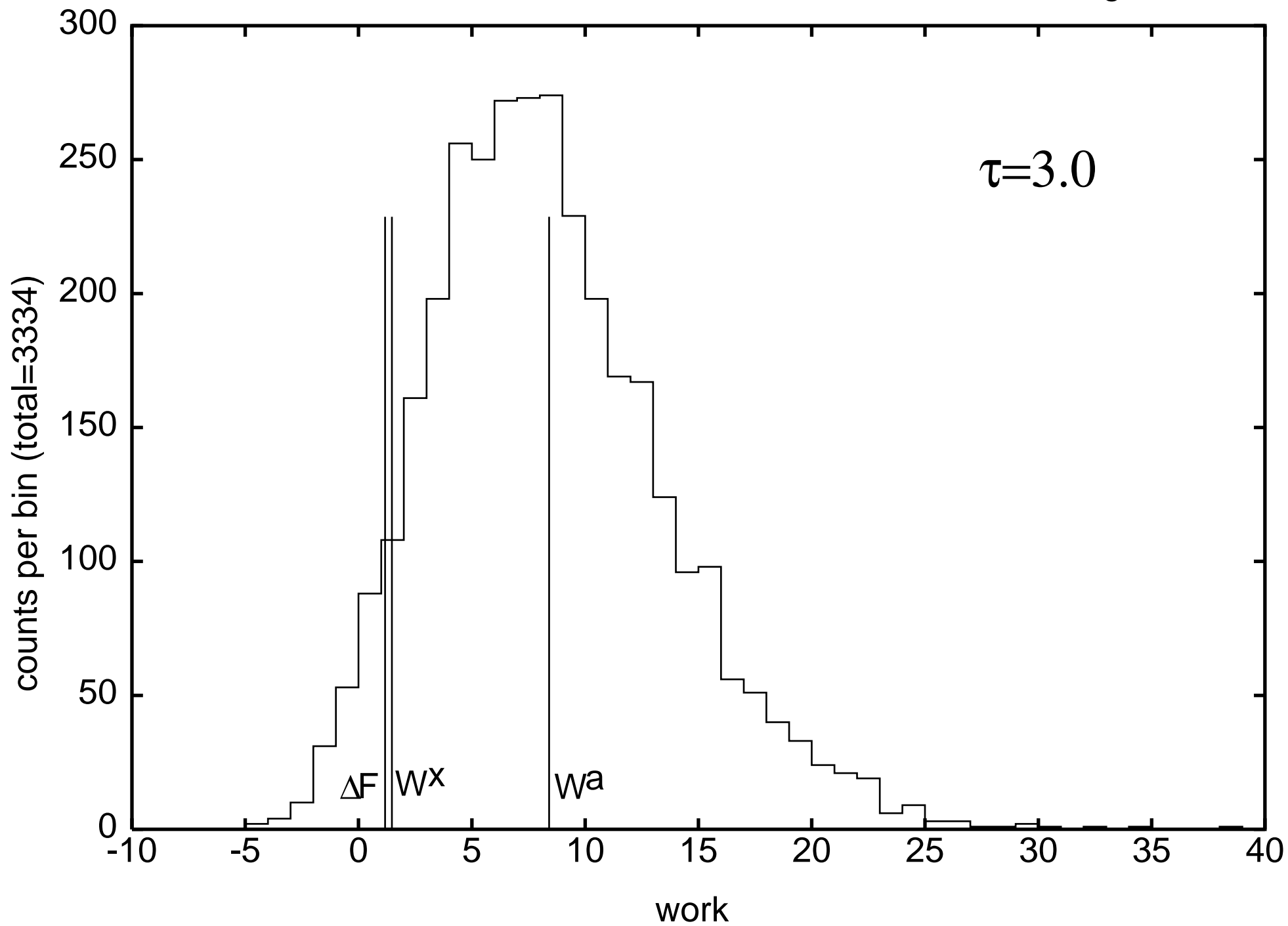


Figure 3

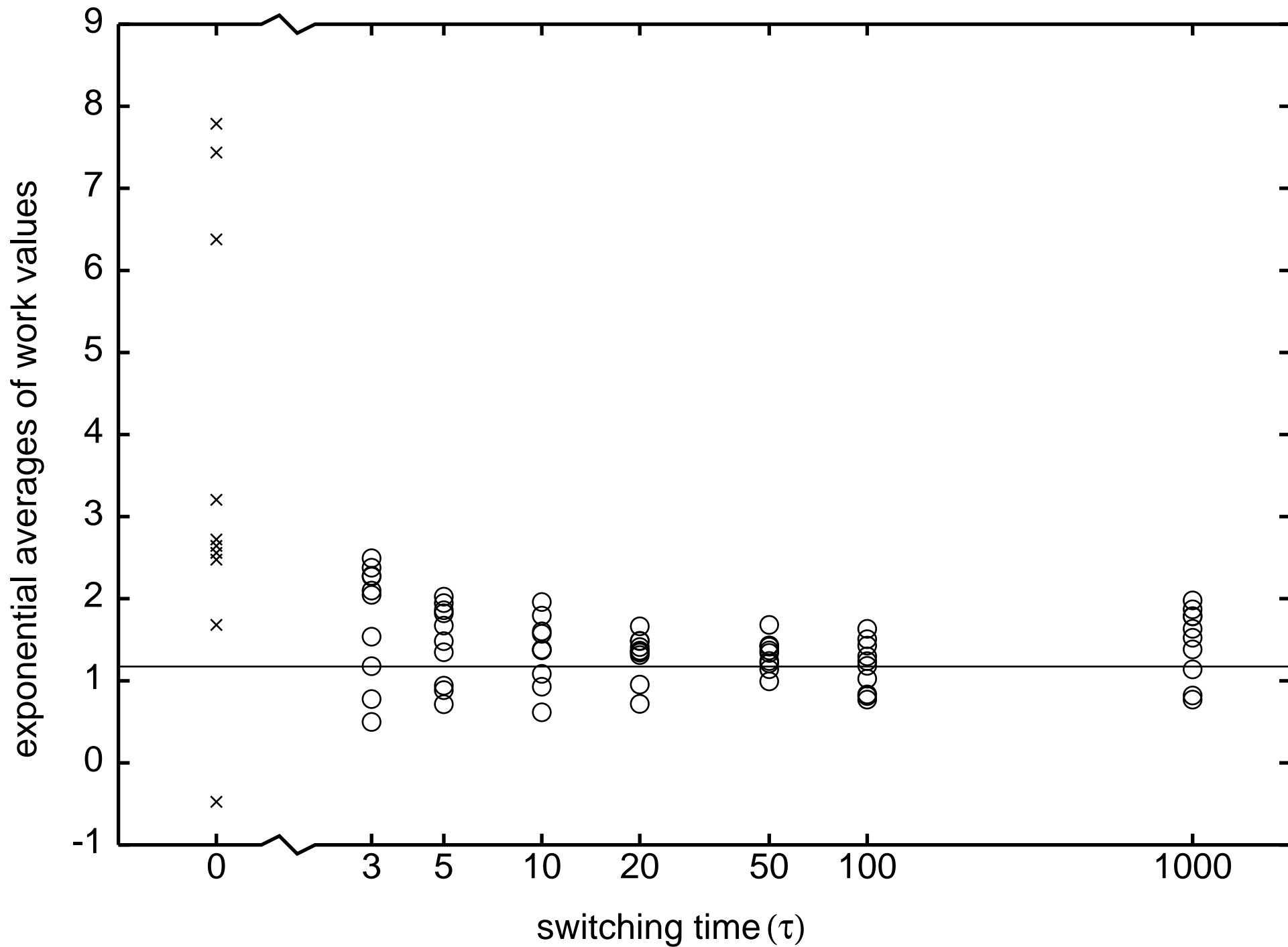


Figure 4

